Nanofabrication (2022) 7, 116-127
https://doi.org/10.37819/nanofab.007.198

eurasia

RESEARCH ARTICLE

Check for updates

A nano-enclatherated-gel-composite for the treatment of alcohol abuse and addiction

Fatema Mia, Mershen Govender, Sunaina Indermun, Pradeep Kumar, Lisa C. du Toit, Yahya E. Choonara*

Wits Advanced Drug Delivery Platform Research Unit, Department of Pharmacy and Pharmacology, School of Therapeutic Sciences, Faculty of Health Sciences, University of the Witwatersrand, Johannesburg, 7 York Road, Parktown 2193, South Africa
**Corresponding Author: Professor Yahya E. Choonara; Tel: +27-11-717-2052; Fax: +27-11-642-4355. Email: Yahya.Choonara@wits.ac.za*

ABSTRACT

Alcoholism is a highly prevalent disease, with successful rehabilitation being poor due to irrepressible cravings that result in relapse. This study developed and analysed an intramuscular injection capable of providing a sustained release of disulfiram over one month. Statistically optimized disulfiram-loaded nanomicelles were prepared and incorporated into a thermosensitive gel resulting in a nano-enclatherated-gel-composite (NEGC). The nanomicelle system demonstrated a drug loading capacity and entrapment efficiency of 33.66% and 50.98%, respectively, with a sustained release of 65% of the administered disulfiram achieved after 28 days through the thermosensitive hydrogel. Additionally, *ex vivo* release studies have been undertaken using rat muscle tissue with *in vivo* biodistribution, plasma levels, histopathology and myotoxicity following oral disulfiram administration and intramuscular NEGC administration also assessed in Sprague-Dawley rats. Results obtained in this study have indicated that the designed delivery system has the potential to successfully release disulfiram in a sustained manner for the treatment of alcohol abuse.

ARTICLE HISTORY:
Received: 9-02-2021
Revised: 27-05-2022
Accepted: 12-06-2022

KEYWORDS:
Disulfiram;
Nanomicelles;
Thermosensitive hydrogel;
Alcohol Abuse and Addiction;
Sprague-Dawley rats

1. Introduction

Alcohol addiction, through a dependency on alcohol-containing products, is a chronic condition that has both negative physiological and psychological effects. Alcohol consumption is widespread, with the total alcohol per capita, according to the World Health Organisation (WHO), being 6.4L, with approximately 43.0% of the total population (15+ years) being current consumers of alcohol as of 2016 [1]. Repeated consumption of these substances affects the brain's reward pathways, and other related functions, with biological, psychological, social, and economic consequences. As a result, self-reliant treatment regimens are often ineffective with many patients experiencing impaired cognitive function and behavioral control, even in cases where a clear commitment to abstinence is present, leading to relapse and treatment failure.

Disulfiram has been shown to be an effective treatment for alcohol abuse. However, its inherent gastrointestinal and blood instability

limits its oral delivery in clinical applications. Injectable formulations incorporating disulfiram, while showing positive results, are often difficult to prepare and manufacture due to the drug's highly hydrophobic nature [2]. To augment the treatment process using disulfiram, a dual system has been developed comprising of statistically optimized nanomicelles containing disulfiram dispersed within a thermosensitive gel for intramuscular administration (Fig. 1). The statistically optimized disulfiram-loaded nanomicelles have been prepared with D-α-tocopheryl polyethylene glycol 1000 succinate (TPGS), which were thereafter incorporated into a thermosensitive gel comprising of High Acyl Gellan Gum (HAGG) and Pluronic F127 (PF127), forming a nano-enclatherated-gel-composite (NEGC). The immediate and subsequent sustained release of disulfiram for 28 days intramuscularly was controlled by utilising both free disulfiram drug and the drug-loaded nanomicelles dispersing within the PF127-HAGG gel. The thermosensitive gel was chosen as the delivery platform due to its easy administration and its serving as a vehicle that allows for a solid gel-depot once administered. The developed system incorporating disulfiram is proposed as a suitable platform for the treatment of alcohol abuse. However, there is potential for the system to be used in other areas of substance abuse treatment or any other therapeutic interventions (through modification of the API and formulation constituents), where patient compliance is essential but not routinely or constantly displayed. Extensive *in vitro* characterization has been undertaken on the NEGC system in this study and *ex vivo* and *in vivo* drug release analysis using Sprague-Dawley rats.

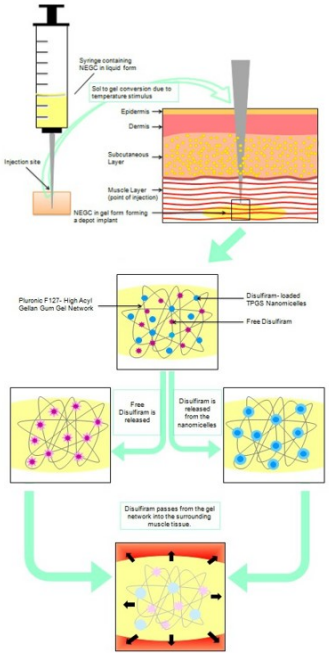

Figure 1. A schematic representation of the administration of the NEGC system and subsequent disulfiram release.

2. Material and methods

2.1. Materials

Tetraethylthiuram disulfide (disulfiram) and Pluronic F127 were procured from Sigma Aldrich (Steinheim, Germany), Kolliphor® TPGS from BASF (Ludwigshafen, Germany) and High Acyl Gellan Gum (Kelcogel LT100) from CP Kelco Germany GmbH (Grossenbrode, Germany). All other chemicals and solvents were of analytic grade and were used as received.

2.2. Disulfiram-loaded TPGS nanomicelles

2.2.1. Preparation of the disulfiram-loaded self-assembled TPGS nanomicelles

Disulfiram-loaded TPGS nanomicelles were prepared by solubilizing disulfiram (100mg) and TPGS (500mg) in chloroform (10mL) on a magnetic stirrer. The polymeric solution was thereafter left overnight in a fume-hood. Deionized water (5mL) was after that added to the residual polymer-drug matrix and stirred for 1 hour resulting in the formation of the nanomicelles. The micellar solution was then transferred to glass petri-dishes and lyophilized. Statistical optimization as well as additional *in vitro* characterization studies on the drug-loaded nanomicelles can be found in the Supplementary Data.

2.2.2. Fourier Transform Infrared Spectroscopy

Elucidation of the structural properties of the native disulfiram and TPGS and the drug-free and disulfiram-loaded nanomicelles was carried out using a Perkin Elmer Spectrum 2000 FTIR spectrometer set 4cm^{-1} resolution and over a 650 to 4000cm^{-1} wavelength.

2.2.3. Determination of the particulate size, zeta potential and distribution

The average particulate size, zeta potential and distribution of the nanomicelles (n=3) were measured using a Zetasizer NanoZS system. All samples were diluted and filtered using a 0.22μm filter before the analysis.

2.2.4. Morphological characterization

The surface morphology of the formulated drug-free and disulfiram-loaded nanomicelles were examined using a carbon-coated copper grid, negatively stained with 1% uranyl acetate in a Transmission Electron Microscope [3].

2.2.5. In vitro *dissolution studies*

In vitro drug release analysis of the disulfiram-loaded nanomicelles (n=3) was undertaken using the dialysis method described by Kulhari and co-workers [4]. Briefly, the nanomicelles were placed in 5mL Simulated Body Fluid (SBF; pH 7.4) within dialysis tubing (MWCO 1000Da). Afterwards, the tube was placed in 50mL SBF at 37°C for 28 days in a shaker bath. At the required periods, samples (1mL) were removed, and diluted with an acetone-buffer solution with the disulfiram content determined using UV spectroscopy (ε = 110.0857 at 262nm).

2.3. Formulation of the NEGC gels

The NEGC gels were formulated by dispersing a combination of 15% PF127 and 0.3% HAGG (PF127-HAGG gel) in deionized water and stirring on a magnetic stirrer at room temperature approximately 3 hours. Once the formulations were fully dissolved, they were transferred to a refrigerator at 10°C for 12 hours [5]. After that, free disulfiram (10mg) and 10mg of disulfiram-loaded nanomicelles were stirred into the PF127-HAGG gel to prepare a uniform dispersion, thereby forming the NEGC gel. FTIR spectroscopy, DSC and XRD of the NEGC gel were assessed as described and can be found in the Supplementary Data. *In vitro* drug release analysis on the NEGC gel was further undertaken as described. Additionally, to ascertain the effect of including both the free disulfiram drug and the disulfiram-loaded nanomicelles, PF127-HAGG gels incorporating free disulfiram and nanomicelles only were investigated for their drug release potential.

2.3.1. Rheological analysis

The amplitude sweep, temperature sweep, frequency sweep, time sweep, and flow analyses of the NEGC gel (0.5mL; n=3) was performed using a Haake Modular Advanced Rheometer System.

2.4. *Ex Vivo* Studies

2.4.1. Ex vivo *drug release study*

Ex vivo disulfiram release from the NEGC system was determined by injecting the NEGC (0.3mL), using a 21G needle, into the excised biceps femoris muscle tissue of a Sprague Dawley rat. The muscle was after that placed at 37ºC for 24 hours in the sample holder of an organ bath, described by Brazeau and Fung [6]. At pre-determined time intervals, samples (1mL) were withdrawn and analyzed using the UV spectroscopy method previously described.

2.5. *In vivo* studies

2.5.1. In vivo *experimental design*

Ethical clearance for this study was obtained from the Animal Ethics Screening Committee (AESC) of the University of the Witwatersrand, South Africa (AESC No. 2014/43/C). All experiments were performed following the relevant regulations.

The *in vivo* evaluation of the disulfiram-loaded NEGC gel was undertaken on 25 Sprague-Dawley rats (250-300g). Before administration, each rat was anesthetized with ketamine (100mg/kg) and xylazine (5mg/kg). Once anesthetized, the disulfiram-NEGC (0.3mL) was injected once-off intramuscularly into the biceps femoris muscle of each rat. Blood samples were extracted from the dosed rats on Days 1, 3, 7, 14, 21 and 28 and analyzed through UPLC. The method used for the UPLC analysis can be found in the Supplementary Data. Biodistribution imaging was further undertaken using the Vevo 2100® Micro Imaging Platform to observe the *in situ* sol-gel transitions of the NEGC gel and to confirm its presence after Day 28.

Two control groups were further employed in addition to the disulfiram-NEGC gel test

group: a comparison group (n=25) that received oral disulfiram daily for 28 days and a placebo group (n=25) that received a once-off drug-free NEGC intramuscular injection containing drug-free nanomicelles. Blood samples were also extracted from each rat in the comparison and placebo groups on Days 1, 3, 7, 14, 21 and 28, with biodistribution imaging also conducted as described. The biceps femoris muscle of each rat was excised after termination for histomorphological analysis.

2.5.1.1. Preparation and administration of the oral disulfiram formulation

Voluntary ingestion was determined as the most practical method of administering oral disulfiram to the rats [7] and was facilitated through the blending of disulfiram into peanut butter dough balls (PBDB) and feeding each rat one PBDB daily for 28 days.

2.5.2. Myotoxicity analysis

Plasma samples from each group were used to quantitatively determine creatine kinase (CK) due to CK being a biochemical marker of muscle injury or damage [8]. Samples of the injected excised biceps femoris muscle tissue were analysed for creatine kinase (CK) presence using a Sigma Aldrich spectrophotometric kit at 340nm as per the manufacturer's standard operating procedure.

2.5.3. Histomorphological analysis of muscle tissue post-IM injection

Histomorphological analysis was undertaken on the muscle tissue harvested after termination to determine if any histomorphological abnormalities were present due to the intramuscular administration of the NEGC system. Before the analysis, each muscle tissue was fixed in 10% normal buffered formalin.

3. Results and Discussion

3.1. Fourier Transform Infrared spectroscopy

Evaluation of the native disulfiram FTIR spectrum noted two peaks at 2975cm^{-1} signifying C-H (CH_3) stretching (peak 1) and at 1493cm^{-1} (peak 2) due to C-H symmetrical deformation vibrations (Fig. 2). Peaks identified between 1345-1455cm^{-1} (peak 4 - peak 3) resulted from CH_2-CH_3 vibrations with C=S stretching, resulting in peak five displayed at 1272cm^{-1}. Peak 6 indicated at 1193cm^{-1} could be attributed to C-H skeletal vibrations can be observed with peak seven at 1150cm^{-1} due to C-C skeletal vibrations. Additionally, the bands identified between 965-1060cm^{-1} (peak 9 - peak 8) were assigned to C-N stretching, while the bands between 816-912cm^{-1} (peak 11 - peak 10) could be attributed to C-S stretching. A comparative evaluation between the native disulfiram and the disulfiram-loaded nanomicelles noted that the characteristic

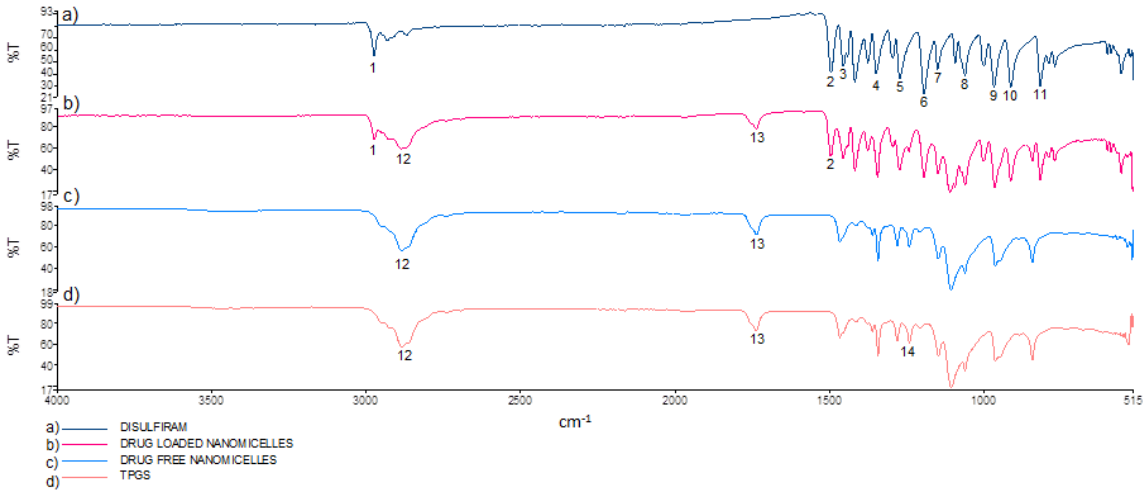

Figure 2. FTIR spectra of **(a)** disulfiram, **(b)** the disulfiram-loaded nanomicelles, **(c)** the drug-free nanomicelles and **(d)** TPGS.

peaks 1 and 2 were still present, indicating the stability of the disulfiram in the formulation.

In addition, peak 12 (2884cm^{-1}) displayed C-H stretching of the CH3 present in the TPGS molecule, while the carbonyl band identified at 1736cm^{-1} (peak 13) further indicated C=O stretching and vibration. The peaks displayed around 1250cm^{-1} (peak 14) can be assigned to C-O stretching. A comparative evaluation of the native TPGS spectrum to the drug-free nanomicelle demonstrated highly similar ranges with minimal variations detailing the stability of the TPGS molecule.

3.2. Analysis of the nanomicelle size and zeta potential

The drug-free and the drug-loaded nanomicelles were evaluated for their particle size, zeta potential and PDI (Table 1, n=3). The zeta size and potential were determined to be 21.61nm and -52.0mV and 23.16nm and 26.4mV for the disulfiram-loaded and drug-free nanomicelles respectively. The smaller size achieved for the drug-free nanomicelles can be attributed to the interaction between the polymer's hydrophobic chains, resulting in a more compact structure [9]. The sizes achieved were within the range to penetrate small capillaries (10nm-70nm), thereby increasing drug circulation, while the zeta potential values reached detailed the formation of a highly stable micellar arrangement [10]. The small size further conceals the nanoparticles from detection by the immune system, protecting them from destruction. Additionally, while disulfiram is known to cross the blood-brain barrier (BBB), the achieved particle size of around 20nm is well within the 100-150nm range required for the nanoparticulate systems to cross the BBB, through the various cellular transport mechanisms of the BBB, for the delivery of other APIs with low BBB permeability [11-13]. The PDI values for both nanomicelles are additionally within the acceptable range.

3.3. Morphological characterization

The shape of the prepared nanomicelles was observed to be spherical and homogenous, as is depicted in the size uniformity present in Fig. 3. The sizes of the particles observed are very similar to those obtained through the DLS analysis. It was further observed that the incorporation of disulfiram into the nanomicelles (Fig. 3a) did not alter the particle morphology. Further noted was that the drug-loaded nanomicelles were well dispersed in the images, which can be attributed to their large zeta potential hindering particulate agglomeration. Conversely, slight agglomeration was determined for the prepared drug-free nanomicelles (Fig. 3b).

Formulation	Size (nm)	PDI	Zeta Potential (mV)
Drug free nanomicelles	23.16 (SD ≤ 10.95)	0.37 (SD ≤ 0.12)	-26.4 (SD ≤ 4.20)
Disulfiram-loaded nanomicelles	21.61 (SD ≤ 6.86)	0.31 (SD ≤ 0.10)	-52.0 (SD ≤ 3.90)

Table 1. Particle size, PDI and zeta potential for disulfiram-loaded and drug-free nanomicelles.

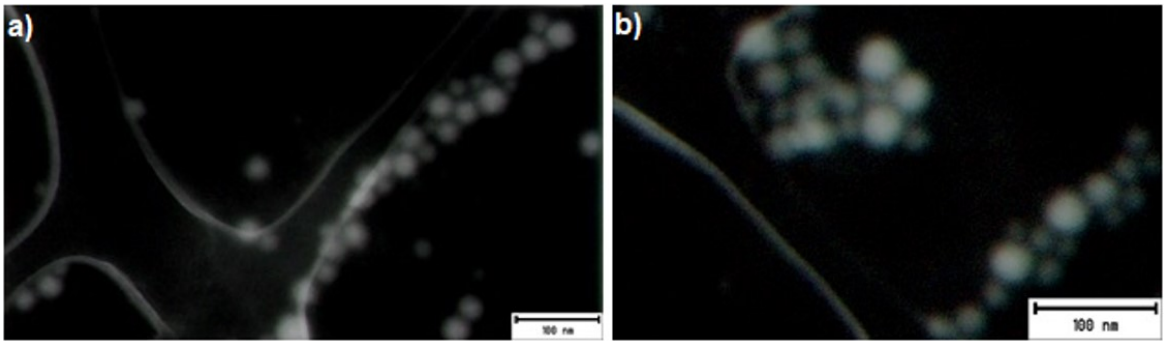

Figure 3. Electron micrographs of **(a)** the disulfiram-loaded nanomicelles and **(b)** the drug free nanomicelles at 50 000x magnification.

3.4. *In vitro* drug release analysis

The *in vitro* disulfiram release profile of the drug-loaded nanomicelles before inclusion in the PF127-HAGG gel displayed a release of 65% disulfiram from the system in 28 days (Fig. 4-Curve A). The initial burst release seen in the profile (12%), within the first 2-4 hours, is due to the relatively high concentration of drug under the surface of the nanomicelles released immediately upon exposure to the dissolution media or to a small quantity of unencapsulated drug that adhered to the nanomicelle outer shell [14,15]. However, the large proportion of drug was firmly incorporated within the nanomicellular inner core, resulting in a slower release profile.

Disulfiram release from the PF127-HAGG gel containing drug-loaded nanomicelles only (curve B) verified that the prepared system does slow the release of disulfiram which can be attributed to the strong complex formed between the two gel-forming polymers. The release rate was noted to decrease by approximately 25% when the drug-loaded nanomicelles were incorporated in the PF127-HAGG gel. Incorporating free disulfiram into the nanomicelle-PF127-HAGG gel system results in an interesting effect, whereby the free disulfiram stabilizes drug release from the drug-loaded nanomicelles. This can be seen in the release profile of curve D and can be attributed to the equilibrium formed between the free disulfiram and the disulfiram within the nanomicellular structure. Evaluation of the gel system containing free disulfiram + the PF127 and HAGG (Curve C) further reflected the effect of dual incorporation of disulfiram, where the release of disulfiram after 28 days (18%) was more than that of the free disulfiram + nanomicelle system (11%). A similar initial release profile of disulfiram was noted for Curves C and D in the first seven days, further highlighting the stabilizing effect of the free disulfiram on the release of the drug from the nanomicelles. Projected calculations revealed that 100% disulfiram release would occur approximately 46 days, 79 days, 176 days, and 303 days for profiles A, B, C, and D. The NEGC system composed of the disulfiram-loaded nanomicelles, and free disulfiram was, therefore, determined to produce the most extended release of disulfiram when compared to other formulation variants. When compared to previous research undertaken, the prepared nanomicelles released disulfiram slower than the disulfiram-loaded redox-sensitive shell crosslinked micelles developed by Duan *et al*. [16], where despite the larger size of the particles (≈80nm), drug loading was only 7.5%, with an *in vitro* release of 84.5% achieved within 24 hours. A similar trend was seen in the study by Miao *et al*. [17], who developed mixed micelles of 86.4 ±13.2nm with a drug loading capacity of

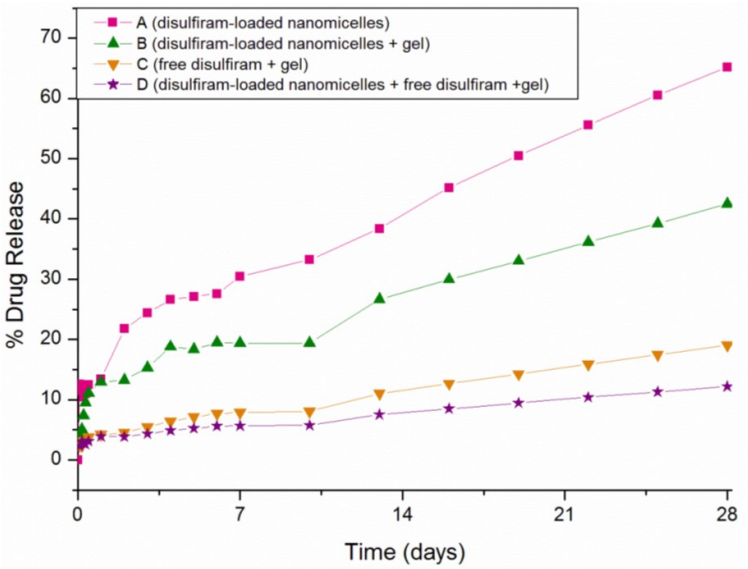

Figure 4. Disulfiram release profiles of **(A)** the disulfiram-loaded nanomicelles, **(B)** the disulfiram-loaded nanomicelles within the PF127 and HAGG gel, **(C)** free disulfiram within the PF127 and HAGG gel and **(D)** the disulfiram-loaded nanomicelles and free disulfiram within the PF127 and HAGG gel (SD ≤ 0.7 in all cases, n=3).

5.90% and an ≈80% disulfiram *in vitro* release in 72 hours. It, however, should be noted that in both studies, the application for the delivery system was for antitumor activity using different polymers than that of the NEGC system.

3.5. Rheological analysis of the gel composites

Rheological evaluation of the PF127 and HAGG gel incorporating the disulfiram-loaded nanomicelles and free disulfiram detailed a decrease in the Kairotic Point (KP) of the formulation (Fig. 5). The KP for the formulation (21.5°C) was acceptable as it allows for rapid transition of the mixture upon intramuscular administration. Furthermore, at lower temperatures, the viscosity of the solution decreased, which would allow for easier injectability.

Evaluation of the gelation time for the PF127 and HAGG gel and the NEGC formulation was noted at a desirable <30 seconds for both formulations (Table 2). The 28.9 second transition time for the NEGC formulation was considered excellent and was much quicker than the 2 minutes reported for a 15% PF127 gel [18]. The gelation time is also advantageous due to long transition periods resulting in the burst release of drugs [19].

The flow behavior index for the PF127 and HAGG gel and the NEGC formulation was <1, signifying shear-thinning behavior in both formulations, which has been noted to promote the injectability of gels [20].

3.6. Ex vivo *drug release*

The *ex vivo* disulfiram release profile of the NEGC system (Fig. 6) showed an initial burst release of disulfiram within one hour (24%), after which the rate of drug release decreased to 44% in 24 hours. The difference in drug release compared to the *in vitro* release profile can be attributed to the size of the muscle sample used, resulting in saturation with the NEGC system, leading to a faster drug release rate.

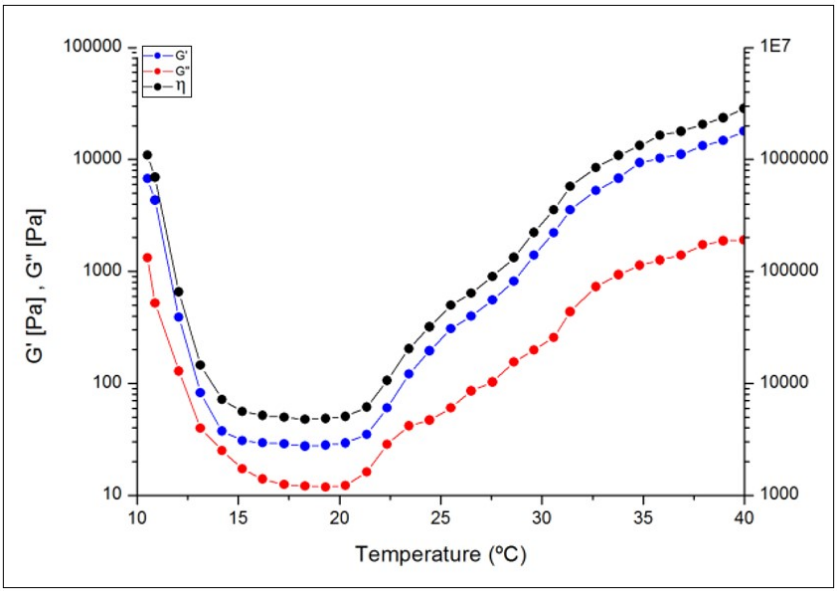

Figure 5. A Temperature Sweep profile of the NEGC gel over a temperature range of 10ºC and 40ºC highlights a decreased viscosity at room temperature and an increased viscosity at physiological temperature.

Formulation	Gelation Temperature (°C)	Gelation Time (seconds)	Flow Curve Model (10°C)	Flow Curve Model (37.5°C)	Flow Behaviour Index
PF127-HAGG gel	25.5	17.00	Cross	Herschel-Bulkley	0.6383
PF127-HAGG + free disulfiram + disulfiram-loaded nanomicelles	21.5	28.90	N/A	Herschel-Bulkley	0.5366

Table 2. Summary of gelation temperature, gelation time and flow curve behavior of the PF127 and HAGG gel and the NEGC formulation.

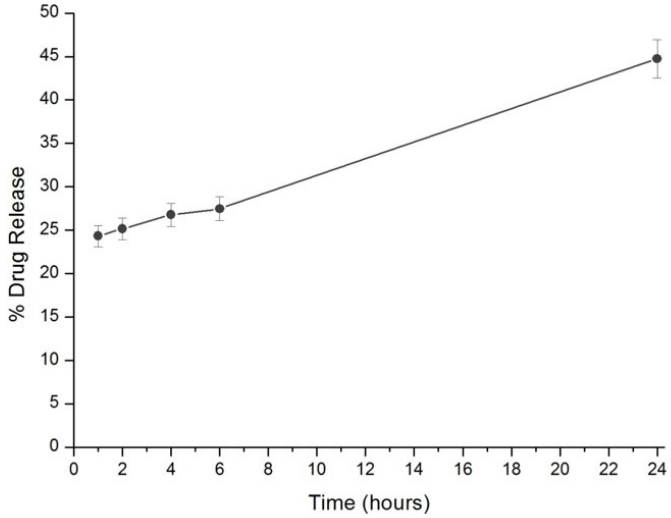

Figure 6. The *ex vivo* drug release profile of the NEGC formulation administered to the excised biceps femoris muscle tissue of a Sprague Dawley rat (SD≤1.24, n=3).

3.7. High-frequency ultrasound imaging

As can be seen in Figures 7A-L, the administered NEGC was visible throughout the 28-day study in both the drug-loaded test group and the drug-free placebo group. It was therefore determined that the NEGC system was retained at the administration site over the test period. A direct echogenicity comparison of the NEGC and standard rat muscle fibers can be found in Fig. 8.

3.8. In vivo *drug release profiles*

Analysis of the *in vivo* release profiles (Fig. 9) detailed that the NEGC (test group) displayed a typical sustained-release curve with peak drug levels achieved after 21 days (27.33µg/mL). Minimum plasma concentration of disulfiram from the test group was further noted to be 1.94ng/mL, with the maximum concentration being 27.33µg/mL. The concentrations achieved were reported as above the minimum therapeutic range of 0.05µg/mL-0.4µg/mL [21]. The comparison group displayed increased plasma concentration, attributed to the half-life disulfiram (60-120 hours), far less than the release rate from the dosed disulfiram-loaded peanut butter balls. The plasma disulfiram concentrations from the test group were similarly lower than the comparison group, attributed to the difference in dosages used. No further fluctuations in disulfiram release were observed. Analysis of the placebo group revealed that no disulfiram was detected over the test period.

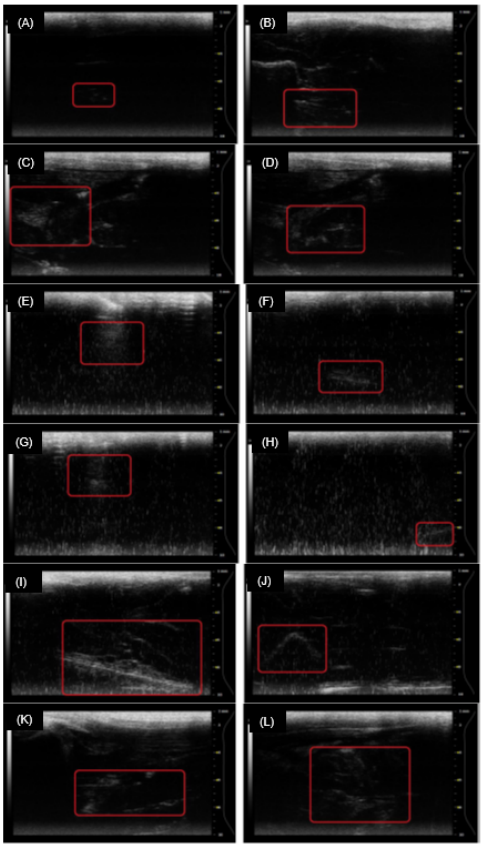

Figure 7. Biodistribution imaging of the drug-free and drug-loaded NEGC respectively in **(A)** and **(B)** 1 hour after administration, **(C)** and **(D)** 24 hours after administration, **(E)** and **(F)** 7 days after administration, **(G)** and **(H)** 14 days after administration, **(I)** and **(J)** 21 days after administration and **(K)** and **(L)** 28 days after administration.

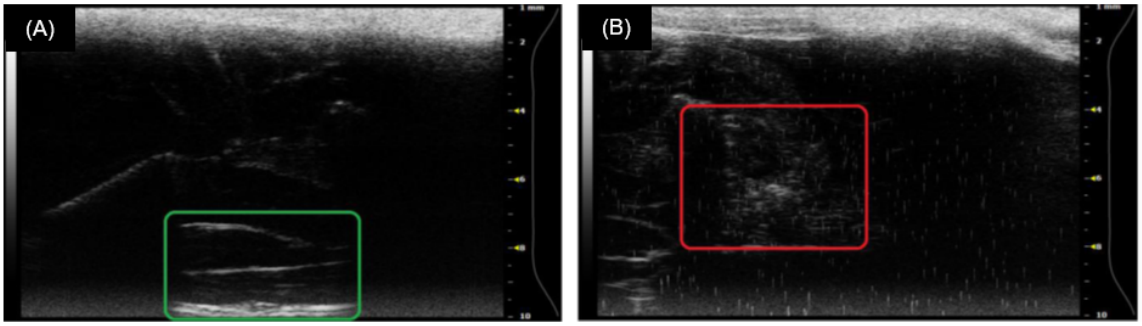

Figure 8. Ultrasound images display **(a)** healthy muscle fibers and **(b)** the *in situ* gel system.

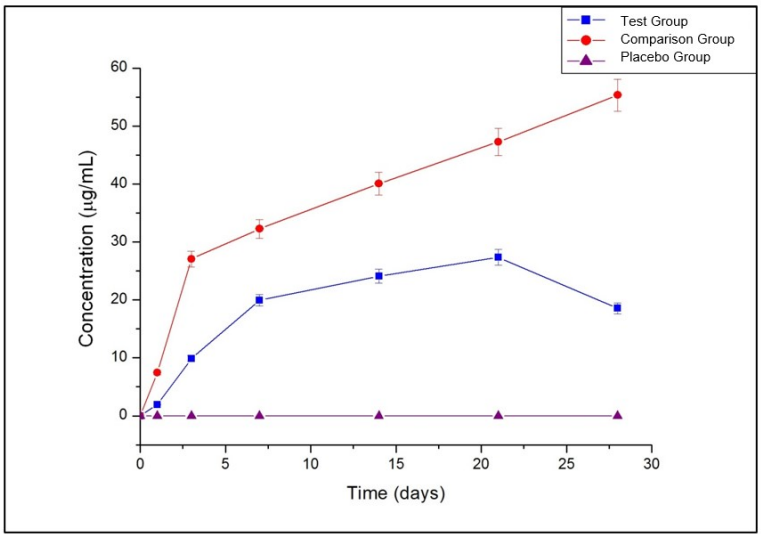

Figure 9. *In vivo* disulfiram release profiles of the test, comparison and placebo groups (SD≤ 1.86 in all cases, n=5).

Previous research has shown that many clinical trials involving disulfiram depots have displayed a lack of efficacy due to insignificant absorption of disulfiram from the administered implant or an inadequate amount of disulfiram reaching systemic circulation to have an effect [22]. Through this *in vivo* drug release study, it was evident that the quantity of drug and rate of release detected after administration of the NEGC system is a significant achievement and further proves the success of the formulation.

3.9. In vivo *myotoxicity*

Myotoxicity of the NEGC system was determined by detecting the CK levels in rat's administered with the system. Evaluation of the placebo group showed normal CK levels (678µ/L) after 2 hours, increasing after 2-6 hours and after that decreasing back to normal range (Fig. 10). The results obtained are following those reported by

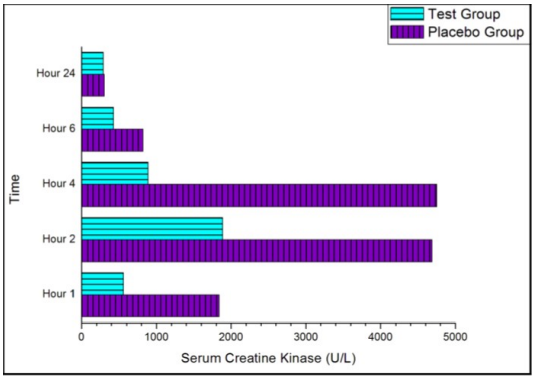

Figure 10. *In vivo* CK levels measured for the test group and placebo group.

Brazeau and Fung [6] and Rungseevijitprapa and co-workers [23]. Brazeau and Fung witnessed low CK release up to 2 hours and a marked increase within 2-4 hours, while Rungseevijitprapa *et al*. noted that peak levels occurred around 2 hours and returned to average 6 hours post-injection. After

6 hours there was no further increase in CK up to 24 hours in this study. Therefore, the increase in enzyme activity is due to the test preparation without significant muscle damage [24]. The results indicate that no permanent damage had occurred after the administration of the NEGC system.

3.10. Histopathological evaluation of muscle tissue

A comparative analysis of the test and placebo groups determined no significant histopathological differences between the groups, demonstrating that the administered disulfiram was not exclusively responsible for any variations seen (Fig. 11). Additionally, no significant toxicity was seen in the first hour for the NEGC test group. Histopathological changes were further seen in the test group between 2 hours to 7 days, while the placebo group showed alterations between Days 1 and 7. In both groups, toxicity levels dropped after Day 7.

In the placebo group, minimal edema and hyaline degeneration were present after 1 hour with mild increases in extravascular mast cells. The presence of an amorphous substance was additionally noted in the perimysium between the muscle fibers. After 2 hours post-administration, the test group showed minimal hemorrhage edema, myofiber fragmentation and inflammation. The placebo group additionally displayed mild edema in the perimysium and surrounding peripheral nerves with minimal hyaline degradation of the scattered fibers.

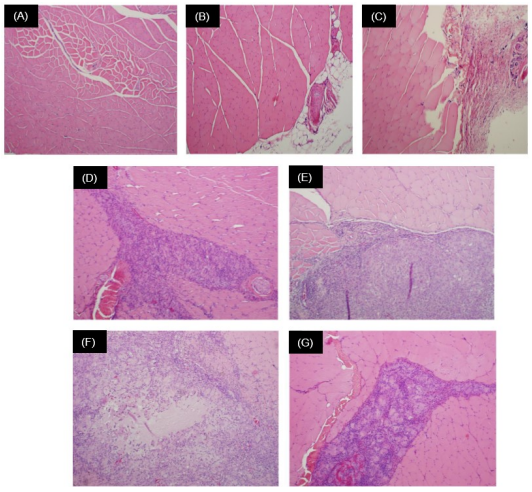

Figure 11. Light microscopy histological images of **(A)** healthy muscle tissue, **(B:** Test Group and **C:** placebo group) muscle tissue with minimal histopathological lesions, **(D:** test group and **E:** placebo group) muscle tissue with mild histopathological lesions and **(F:** test group and **G:** placebo group) muscle tissue with moderate histopathological lesions.

After 24 hours, mild edema, fibrin deposition, fragmentation and inflammation were present in both groups, while minimal edema was noted with an increase in inflammation in the test group with moderate edema and inflammation in the placebo group after two days. After 7 days, moderate inflammation and edema with minimal fibrosis and mild fragmentation were seen in the test group with the placebo group similar, except for moderate fibrosis and no fragmentation. After 14 days of administration, inflammation was moderate in both groups, with fragmentation absent. Both groups displayed a significant decrease in histopathological variations between 7 and 14 days. After 21 days, minimal fibrosis and an area of mild macrophage infiltration were present in the test group, with the placebo group showing moderate fibrosis and inflammation with minimal degeneration. After 28 days, the test group displayed mild inflammation, degeneration, fibrosis, and fragmentation with no further changes in the placebo group since Day 21. The histopathological results indicated acute toxicity and mild muscle tissue injury consistent with needle insertion and rapid administration of the formulation [25,26].

4. Conclusion

The developed NEGC system was successfully prepared and evaluated *in vitro*, *ex vivo* and *in vivo* in this study. *In vitro* analysis detailed the morphological, rheological and structural properties of the constituents of the NEGC system and the benefit of using both free drug and drug-loaded nanomicelles within the system (11% disulfiram release within 28 days of administration compared to 42% release from the nanomicelles within the thermoresponsive gel alone) with *in vivo* analysis showing that after administration of the NEGC system to rats via IM injection, the NEGC system released disulfiram over the 28-day test period in a sustained release manner with a maximum plasma disulfiram concentration achieved after 21 days (27.33µg/mL). The presence of the NEGC system in the rat body after 28 days was further confirmed through

high-frequency ultrasound imaging with myotoxicity and histopathology studies displaying acute toxicity common in IM administration of the drug-loaded and drug-free gels with all significant histopathological abnormalities decreasing 7 days after administration of the system. *In vivo* analyses furthermore highlight the therapeutic potential of the NEGC system, whereby a patient could be administered with the system every few weeks with little need for patient compliance. This would have several benefits in alcohol dependence and other therapeutic interventions whereby the API and formulation constituents can be modified to ensure increased patient adherence and improved treatment outcomes.

Research funding

This research work was funded by the National Research Foundation (NRF) of South Africa.

Author contribution

Fatema Mia performed the initial research investigation, and method development and wrote the original draft of the research paper. Mershen Govender and Sunaina Indermun undertook subsequent research and conducted a review and editing of the research paper. Pradeep Kumar, Lisa du Toit and Yahya Choonara conceptualized the project and supervised the completion of the research paper.

Conflicts of Interest

The authors state no conflict of interest.

References

1. WHO, 2018. Global status report on alcohol and health. https://apps.who.int/iris/bitstream/handle/10665/274603/9789241565639-eng.pdf (accessed 01 September 2021).
2. Chen X, Zhang L, Hu X, Lin X, Zhang Y, Tang X. Formulation and preparation of a stable intravenous disulfiram-loaded lipid emulsion. Eur J Lipid Sci. Technol. 2015;117(6):869-78. doi:10.1002/ejlt.201400278.
3. Lu J, Huang Y, Zhao W, Marquez RT, Meng X, Li J, et al. PEG-derivatized embelin as a nanomicellar carrier for delivery of paclitaxel to breast and prostate cancers. Biomaterials 2013;34(5):1591-1600. doi:10.1016/j.biomaterials.2012.10.073.
4. Kulhari H, Pooja D, Shrivastava S, Telukutala SR, Barui AK, Patra CR, et al. Cyclic-RGDfK peptide conjugated succinoyl-TPGS nanomicelles for targeted delivery of docetaxel to integrin receptor over-expressing angiogenic tumours. Nanomedicine 2015;11(6):1511-20. doi:10.1016/j.nano.2015.04.007.
5. Ricci EJ, Lunardi LO, Nanclares DMA, Marchetti JM. Sustained release of lidocaine from Poloxamer 407 gels. Int J Pharm. 2005;288(2):235-44. doi:10.1016/j.ijpharm.2004.09.028.
6. Brazeau GA, Fung HL. An in vitro model to evaluate muscle damage following intramuscular injections. Pharm Res. 1989; 6(2):167-70. doi:10.1023/a:1015940811827.
7. Diogo LN, Faustino IV, Afonso RA, Pereira SA, Monteiro EC, Santos AI. Voluntary Oral Administration of Losartan in Rats. J Am Assoc Lab Anim Sci. 2014;54(5):549-56.
8. Brancaccio P, Lippi G, Maffulli N. Biochemical markers of muscular damage. Clin Chem Lab Med. 2010;48(6):757-67. doi:10.1515/CCLM.2010.179.
9. Butt AM, Amin MCIM, Katas H, Sarisuta N, Witoonsaridsilp W, Benjakul R. In vitro characterization of pluronic F127 and D-α-tocopheryl polyethylene glycol 1000 succinate mixed micelles as nanocarriers for targeted anticancer-drug delivery. J Nanomater. 2012;916573. doi:10.1155/2012/916573.
10. Goldberg M, Langer R, Jia X. Nanostructured materials for applications in drug delivery and tissue engineering. J Biomater Sci Polym Ed. 2007;18(3):241-68. doi:10.1163/156856207779996931.
11. Kumar R, Aadil KR, Mondal K, Mishra YK, Oupicky D, Ramakrishna S, Kaushik A. Neurodegenerative disorders management: state-of-art and prospects of nano-biotechnology. Crit Rev Biotechnol. 2021;25:1-33. doi:10.1080/07388551.2021.1993126.
12. Nehra M, Uthappa UT, Kumar V, Kumar R, Dixit C, Dilbaghi N, Mishra YK, Kumar S, Kaushik A. Nanobiotechnology-assisted therapies to manage brain cancer in personalized manner. J Control Release. 2021;338:224-43. doi: 10.1016/j.jconrel.2021.08.027.

13. Kaushik A, Jayant RD, Bhardwaj V, Nair M. Personalized nanomedicine for CNS diseases. Drug Discov Today. 2018;23(5):1007-15. doi: 10.1016/j.drudis.2017.11.010.
14. Mi Y, Zhao J, Feng SS. Vitamin E TPGS prodrug micelles for hydrophilic drug delivery with neuroprotective effects. Int J Pharm. 2012;438(1):98-106. doi:10.1016/j.ijpharm.2012.08.038.
15. Mu L, Elbayoumi TA, Torchilin VP. Mixed micelles made of poly (ethylene glycol)–phosphatidylethanolamine conjugate and d-α-tocopheryl polyethylene glycol 1000 succinate as pharmaceutical nanocarriers for camptothecin. Int J Pharm. 2005;306(1):142-9. doi:10.1016/j.ijpharm.2005.08.026.
16. Duan X, Xiao J, Yin Q, Zhang Z, Yu H, Mao S, Li Y. Multi-targeted inhibition of tumor growth and lung metastasis by redox-sensitive shell crosslinked micelles loading disulfiram. Nanotechnology. 2014;25(12):125102. doi:10.1088/0957-4484/25/12/125102.
17. Miao L, Su J, Zhuo X, Luo L, Kong Y, Gou J, Yin T, Zhang Y, He H, Tang X. mPEG5k-b-PLGA2k/PCL3.4k/MCT Mixed Micelles as Carriers of Disulfiram for Improving Plasma Stability and Antitumor Effect in Vivo. Mol. Pharm. 2018;15(4):1556-64. doi:10.1021/acs.molpharmaceut.7b01094.
18. Kojarunchitt T, Hook S, Rizwan S, Radesa T, Baldursdottir S. Development and characterization of modified poloxamer 407 thermoresponsive depot systems containing cubosomes. Int J Pharm. 2011;408(1):20-6. doi:10.1016/j.ijpharm.2011.01.037.
19. Avachat AM, Kapure SS. Asenapine maleate in situ forming biodegradable implant: An approach to enhance bioavailability. Int J Pharm. 2014;477(1):64-72. doi:10.1016/j.ijpharm.2014.10.006
20. Kapoor DN, Katare OP, Dhawan S. In situ forming implant for controlled delivery of an anti-HIV fusion inhibitor. Int J Pharm. 2012;426(1):132-143. doi: 10.1016/j.ijpharm.2012.01.005.
21. Saracino MA, Marcheselli C, Somaini L, Gerra G, De Stefano F, Pieri MC, et al. Simultaneous determination of disulfiram and bupropion in human plasma of alcohol and nicotine abusers. Anal Bioanal Chem. 2010;398(5):2155-61. doi:10.1007/s00216-010-4172-z.
22. Hegde A, Singh SM, Sarkar S. Long-acting Preparations in Substance Abuse Management: A Review and Update. Indian J Psychol Med. 2013;35(1):10-18. doi:10.4103/0253-7176.112194.
23. Rungseevijitprapa W, Brazeau GA, Simkins JW, Bodmeier R. Myotoxicity studies of O/W-in situ forming microparticle systems. Eur J Pharm Biopharm. 2008;69(1):126-33. doi:10.1016/j.ejpb.2007.10.009.
24. Surber C, Sucker H. Tissue tolerance of intramuscular injectables and plasma enzyme activities in rats. Pharm Res. 1987;4(6):490-4. doi:10.1023/a:1016427605545.
25. Sluka KA, Kalra A, Moore SA. Unilateral intramuscular injections of acidic saline produce a bilateral, long-lasting hyperalgesia. Muscle Nerve 2001;24:37-46. doi:10.1002/1097-4598(200101)24:1<37::aid-mus4>3.0.co;2-8.
26. Thuilliez C, Dorso L, Howroyd P, Gould S, Chanut F, Burnett R. Histopathological lesions following intramuscular administration of saline in laboratory rodents and rabbits. Exp Toxicol Pathol. 2009;61(1):13-21. doi:10.1016/j.etp.2008.07.003.